Steroid receptor co-activator interacting protein (SIP) mediates EGF-stimulated expression of the prostaglandin synthase COX2 and prostaglandin release in human myometrium

Claire A. Hudson[1*], Craig A. McArdle[1], Andrés López Bernal[1, 2]

[1]University of Bristol, School of Clinical Sciences, Dorothy Hodgkin Building, Whitson Street, Bristol, BS1 3NY, UK.

[2]Department of Obstetrics and Gynaecology, St Michael's Hospital, Southwell Street, Bristol, BS2 8EG, UK.

Running Title: EGF-induced expression of COX2 requires SIP

*** Corresponding Author:** Claire A Hudson, email: claire.hudson@bristol.ac.uk

Abstract

Study hypothesis: Steroid receptor coactivator interacting protein (SIP/KANK2) is involved in regulating the expression of the prostaglandin (PG)-endoperoxide synthase 2 (PTGS2; also known as cyclo-oxygenase 2, COX2) and PG release in human myometrium.

Study finding: SIP is phosphorylated in myometrial cells in response to epidermal growth factor (EGF)-stimulation and is required for EGF-stimulated increases in COX2 expression, PGE_2 and $PGF_{2\alpha}$ release, and expression of interleukins (IL) 6 and IL8.

What is known already: Human parturition involves inflammatory and non-inflammatory pathways and requires activation of the intrauterine PG cascade. A key mediator of uterine PG production is the highly inducible enzyme COX2. Regulation of COX2 expression is complex, and novel factors involved in its induction may play an important role during labour. The expression and function of SIP in uterine tissues has never been investigated.

Study design, samples/materials, methods: Mass spectrometry was used to identify SIP from cultured primary myometrial cells, and its expression in fresh placenta, fetal membranes, decidua and myometrium from pregnant and non-pregnant women was determined by western blotting. SIP expression in myometrial cells was reduced using small interfering RNA (siRNA), and COX2 expression was stimulated with EGF. *COX2, IL6* and *IL8* mRNA and COX2 protein expression were measured using quantitative RT-PCR (RT-qPCR) and western blotting respectively, and release of PGE_2 and $PGF_{2\alpha}$ by enzyme immunoassay. The time course and dose response of SIP phosphorylation in response to EGF were determined, and phosphorylation was measured in the presence of the mitogen-activated protein kinase kinase 1(MEK1) inhibitor PD-184352. Fresh myometrial tissue was used to confirm effects of EGF and MEK1 inhibition on SIP phosphorylation and COX2 expression. A profile of transcription factor (TF) activity after SIP knockdown was carried out using a commercially available array.

Main results and the role of chance: We have demonstrated expression of SIP in human myometrium. siRNA-mediated knockdown of SIP resulted in decreased EGF-stimulated COX2

protein expression ($P < 0.001$), and decreased release of PGE_2 ($P < 0.001$) and $PGF_{2\alpha}$ ($P < 0.01$) . EGF stimulation resulted in rapid and transient phosphorylation of SIP, which was blocked by pharmacological inhibition of the MEK1/ERK (extracellular signal-regulated kinase) signalling pathway with PD-184352 ($P < 0.001$). Moreover inhibition of ERK signalling significantly decreased EGF-stimulated COX2 expression ($P < 0.001$). EGF phosphorylated SIP and increased COX2 expression in a MEK1/ERK-dependent manner in freshly isolated pregnant myometrium. Our data have uncovered a pathway mediating EGF-stimulated COX2 expression that is ERK and SIP dependent, providing a novel function for SIP in the pregnant uterus. Furthermore, EGF stimulated the expression of *IL6* and *IL8* mRNA in a SIP-dependent manner (both $P < 0.05$), and SIP expression was positively associated with activation of serum response factor (SRF) and YY1 TF ($P < 0.001$ and $P < 0.05$ respectively), suggesting additional important roles for myometrial SIP.

Limitations, reasons for caution: While we describe a new role for myometrial SIP, we are yet to determine whether SIP phosphorylation is required for its effects on regulating COX2 expression and PG release. Our data are from *in vitro* studies using fresh tissue and cultured myometrial cells and may not fully reflect the conditions *in vivo*.

Wider implications of the findings: Our group has previously described increases in myometrial COX2 expression with labour at term and preterm. EGF levels rise in the amniotic fluid near term suggesting it may participate in paracrine signalling events, altering gene expression in the myometrium. Our novel data describe a role for SIP in regulating EGF-stimulated expression of myometrial COX2 and PG release. Moreover, our profile of SIP-dependent TF activation provides a platform for further investigations into additional roles for SIP in uterine function. These findings may facilitate the development of new, targeted drugs for the management of labour.

Large scale data: Not applicable.

Study funding and competing interest(s): This work was supported by an Action Medical Research grant (SP4612). The authors have no competing interests to declare.

69

70 **Key Words:** human myometrium; parturition; cyclooxygenase-2; prostaglandin-endoperoxide
71 synthase 2; epidermal growth factor; gene expression; KANK2; steroid receptor co-activator-
72 interacting protein.

73

74

Introduction

Inflammatory responses are an important component of parturition at term and preterm. They involve activation of the intrauterine prostaglandin (PG) cascade, leading to increased uterine PG production at labour. This can be measured as increasing PG levels in amniotic fluid with progressive cervical dilation (Keirse, 1978), and an increase in PG metabolites in maternal serum (Sellers *et al.* , 1982). PGs facilitate concerted cervical ripening, fetal membrane rupture, and the development of myometrial contractions. Consequently, PGs have been used successfully for clinical induction of labour and PG inhibitors for the treatment of preterm labour (Haas *et al.* , 2012, Kaminski *et al.* , 1994). Prostaglandin-endoperoxide synthases 1 and 2 (PTGS1 and 2), also known as cyclo-oxygenases 1 and 2 (COX1 and 2) are rate-limiting enzymes for PG synthesis. They convert arachidonic acid to prostaglandin endoperoxides, which are further converted into a variety of PGs by cell-specific terminal synthases. COX2 is a highly inducible enzyme; in human myometrium COX2 is upregulated in late pregnancy and with labour (Erkinheimo *et al.* , 2000, Phillips *et al.* , 2011, Slater *et al.* , 1999b) whereas COX1 and the terminal PG synthases including PTGDS, PTGES and PGF synthase (AKR1B1) are constitutively expressed (Phillips *et al.*, 2011), hence COX2 is considered a key regulator of PG synthesis during pregnancy and labour. COX2 gene and protein expression in human fetal membranes has been shown to increase during gestation and labour (Slater *et al.* , 1999a), while other studies show an increase in COX2 with gestational age at delivery, without a significant increase with labour in women (Phillips *et al.* , 2014). These increases are thought to be the cause rather than the effect of labour, as increases in COX2 expression (Slater *et al.*, 1999a, Slater *et al.*, 1999b) and amniotic fluid $PGF_{2\alpha}$ levels (Lee *et al.* , 2009) precede labour in women. Expression of COX2 and PG release are further increased in human placenta and fetal membranes in cases of inflammatory infiltration (Lopez Bernal *et al.* , 1989, Phillips *et al.*, 2014), and amniotic fluid levels of PGE_2 and $PGF_{2\alpha}$ increase during preterm labour with underlying intra-amniotic infection (Romero *et al.* , 1987). Uterine COX2 expression can be stimulated by mechanical stretch and by a variety of agonists including pro-inflammatory cytokines e.g. interleukin (IL) 1B and tumor necrosis factor (TNF), oxytocin (OXT), epidermal growth factor (EGF) and PGs themselves (Ackerman *et al.* , 2004, Chen *et al.* , 2012, Mohan *et al.* , 2007, Molnar *et al.* , 1999, Phillips *et al.*, 2011, Sooranna *et al.* ,

2004, Wouters *et al.* , 2014). The signalling pathways mediating agonist-induced increases in COX2 in the late pregnant uterus are complex and not fully elucidated. The COX2 gene promotor contains binding sites for several TFs including nuclear factor kappa B (NFKB), specificity protein 1 (SP1), CCAAT/enhancer-binding protein beta (CEBPB), cAMP response element binding protein (CREB) and peroxisome proliferator-activated receptor gamma (PPARG) (Kang *et al.* , 2007). NFKB activity is important for cytokine-induced increases in COX2, whereas OXT, EGF and PGs signal predominantly through extracellular signal-regulated kinase 1/2 (ERK1/2), protein kinase C (PKC) isoforms or nuclear factor of activated T-cells (NFAT) (Ackerman *et al.*, 2004, Chen *et al.*, 2012, Molnar *et al.*, 1999, Pont *et al.* , 2012, Wouters *et al.*, 2014).

Steroid receptor coactivator (SRC) interacting protein (SIP or KANK2/ ANKRD25) is part of the KANK protein family whose members are characterised by a N-terminal KN motif, coiled-coil domains and C-terminal ankyrin repeat domains (Kakinuma *et al.* , 2009). All family members are thought to regulate actin polymerisation, as overexpression of each disrupts stress fibre formation (Zhu *et al.* , 2008). Akt-dependent phosphorylation of KANK1 results in binding of 14-3-3 proteins and negative regulation of RhoA-dependent actin polymerisation (Kakinuma *et al.* , 2008). In rat kidney, SIP (KANK2) binds Rho GDP-dissociation inhibitor (RhoGDI) which determines its ability to regulate RhoA-GTP levels (Gee *et al.* , 2015). There is evidence that SIP plays an alternative role in regulating estrogen-mediated transcription in MCF-7 cells. SIP functions by binding and sequestering SRC proteins in the cytoplasm, a process that requires Ca^{2+} /calmodulin-dependent protein kinase II (CAMK2)-dependent phosphorylation of SIP (Zhang *et al.* , 2007). Furthermore, mutations in the ankyrin repeat domain relieve cytoplasmic sequestration of SRC proteins and result in increased vitamin D receptor activity and keratoderma (Ramot *et al.*, 2014). An additional role for SIP is regulation of apoptosis through binding to apoptosis-inducing factor in the mitochondria (Wang *et al.* , 2012).

Here we report identification of SIP through mass spectrometry as a myometrial protein that is phosphorylated by EGF. We assessed possible functions for SIP in human pregnant myometrium,

and found that SIP is required for EGF-stimulated expression of COX2, IL6 and IL8, and EGF-stimulated release of PGE_2 and $PGF_{2\alpha}$. EGF-mediated effects on SIP phosphorylation and COX2 induction are dependent on ERK1/2.

Materials and methods

Ethical approval and tissue collection.

This study was approved by the North Somerset and South Bristol Research Ethics Committee (reference E5431) and all women gave informed written consent. Placenta and fetal membranes were collected immediately post-partum from term (≥ 37 weeks gestation) not-in-labour (TNIL) women, delivery by elective caesarean section indicated by previous section and/or breech presentation. Myometrium was collected from the following additional groups of women: preterm (28–36 weeks gestation) not-in-labour (PNIL), delivery by caesarean section for maternal or fetal complications; term following induction of labour (IOL) with intravaginal PGE_2 pessary and/or i.v. OXT infusion with caesarean section; and non-pregnant (NP) taken at hysterectomy in premenopausal women. The tissue was washed in ice-cold isotonic saline and transported to the laboratory where it was used to prepare tissue lysates, tissue explants or freshly dispersed myometrial cells.

Materials.

149 The following chemicals and reagents were obtained from the indicated sources: ON-TARGET plus
150 non-targeting pool small interfering RNA (siRNA) and Dharmafect 1 transfection reagent were
151 purchased from Abgene (Epsom, UK). siRNAs targeting SIP were designed and purchased from
152 Eurofins (London, UK) and Invitrogen, Life Technologies (Stealth Select RNAi™ , Paisley, UK).
153 Collagenase type II, dispase, Dulbecco's modified Eagle's medium (DMEM) and fetal calf serum
154 (FCS) were purchased from Invitrogen, Life Technologies (Paisley, UK); elastase, DNAse, and OXT
155 were purchased from Sigma Aldrich (Poole, UK). Forskolin (FSK) and EGF were purchased from
156 Merck (Nottingham, UK). MEK1 inhibitor PD-184532 was purchased from R&D systems (Abingdon,
157 UK). Myosin light chain kinase (MYLK) (# ab76092), SIP (ANKRD25, # ab99351), glyceraldehyde-
158 3-phosphate dehydrogenase (GAPDH, # ab181602) and COX2 (# ab52237) antibodies were
159 purchased from Abcam (Cambridge, UK); phosphorylated ERK (pERK)1/2 (# 4377) and ERK1/2 (#
160 9102) antibodies were purchased from New England Biolabs (Hitchin, UK); RhoGDI antibody (sc-
161 360) and normal rabbit immunoglobulin (Ig)G (sc-2027) were purchased from Santa Cruz
162 Biotechnology (Heidelberg, Germany). An antibody marketed for detection of phosphorylated MYLK
163 (# 44-1085G) but found actually to recognise phospho-SIP (see Results), was purchased from Life
164 Technologies (Paisley, UK). All other basic chemicals were supplied by Sigma Aldrich (Poole, UK)
165 unless otherwise stated.
166

Myometrial cell culture and stimulation.

Myometrial tissue was digested in serum-free DMEM containing 300 U/ml collagenase (type II), 0.3 U/ml dispase, 30 U/ml DNase I and 0.09 U/ml elastase at 37 °C for 3 hours. Liberated smooth muscle cells were then grown in adherent cell culture with DMEM containing 10 % FCS, 100 U/ml penicillin and 100 µg/ml streptomycin at 37 °C. Experiments were carried out by plating cells of passage seven or lower at $2.8x10^5$ per cm^3 in 12-well plates and growing to confluency over 3 days. For phosphorylation experiments, cells were serum-starved for 4 hours prior to experiments, pre-treated for 30 mins with MEK1 inhibitor where appropriate (PD-184352, 10 µM) followed by stimulation (typically with EGF, 25 ng/ml, 15 mins). For COX2 expression, cells were incubated in phenol red-free and serum-free media for 24 hours in the presence or absence of stimulation (typically 25 ng/ml EGF). In both cases, cells were washed with phosphate-buffered saline (PBS), lysed directly in boiling sodium dodecyl sulphate polyacrylamide gel electrophoresis (SDS-PAGE) sample buffer (25 mM Tris pH 6.8, 10 % glycerol, 2 % SDS, 12.5 mM dithiothreitol (DTT) and 0.002 % bromophenol blue), and used for immunoblotting as described below.

Immunoprecipitation with pMYLK (44-1085G) and SIP antibodies.

Myometrial cells grown to confluency in 10 cm dishes were serum-starved for 4 hours and then treated with or without 10 µM FSK or 25 ng/ml EGF for 15 min.

For pMYLK immunoprecipitates (IPs): Cells were lysed on ice with 350 µl Triton buffer (20 mM Tris-HCl pH 8.2, 400 mM NaCl, 0.5 % Triton X-100, 0.5 mM EDTA, 0.5 mM EGTA, 1 mM DTT, 1x protease (cOmplete) and phosphatase (PhosTOP) inhibitor mix (Roche Diagnositics Ltd, Burgess Hill, UK). Lysates were cleared by centrifugation at 16,000 g for 15 minutes at 4 ˚C and supernatants diluted 1:3 in dilution buffer (20 mM Tris-HCl pH 7.5, 0.5 % Triton X-100, 0.5 mM EDTA, 1 mM DTT and 1x protease and phosphatase inhibitor mix as above). Protein concentration was determined using the BCA assay kit (Perbio Science UK, Cramlington, UK), and approximately 0.5ml of lysate at 1mg/ml was used per IP. Lysates were pre-cleared with protein A and protein G and then incubated with 6 µl/ml anti-phospho-MYLK (Ser1760, 44-1085G) antibody for 2 hours at 4 ˚C with rotation. Immune complexes were captured with 50 µl of each 50 % (v/v) protein A and 50 % (v/v) protein G

for 2 hours at 4 ˚C with rotation. IPs were washed 4 x 1 ml with wash buffer (20 mM Tri-HCl pH 7.7, 0.5 % Triton X-100, 100 mM NaCl, 0.5 mM EDTA, 0.125 mM EGTA and 1 mM DTT) and eluted in SDS-sample buffer (25 mM Tris pH 6.8, 10 % glycerol, 2 % SDS, 12.5 mM DTT and 0.002 % bromophenol blue). 44-1085G IPs were run on 4-12 % NuPAGE Bis-Tris precast gels (Invitrogen Life Technologies, Paisley, UK) which were used for a combination of immunoblotting with the 44-1085G antibody and silver staining to visualise proteins (SilverQuest kit, Invitrogen Life Technologies, Paisley, UK). Following overlay of the 44-1085G immunoblot with the silver-stained picking gel, a gel slice was excised which corresponded to the ~ 100kDa band on the 44-1085G blot. *For SIP IPs:* Cells were lysed on ice in 1 ml SIP IP buffer (20 mM Hepes pH 7.8, 150 mM NaCl, 1 % Triton X-100, 1 mM EDTA, 1 mM EGTA, 1x protease and phosphatase inhibitors as above). Lysates were cleared by centrifugation at 16,000 g for 15 minutes at 4 ˚C and protein concentration was determined using the BCA assay kit and adjusted to 1 mg/ml using SIP IP buffer. Lysates were pre-cleared with protein A and protein G before being divided into 2 x 0.5 ml (500 µg) samples and incubated with either 4 µg of anti-SIP antibody or 4 µg of normal rabbit IgG (control IP) for 2 hours at 4 ˚C with rotation. Immune complexes were captured with 50 µl of each 50 % (v/v) protein A and 50 % (v/v) protein G for 2 hours at 4 ˚C with rotation. IPs were washed 4 x 1 ml with SIP IP buffer and eluted in SDS-sample buffer as above. SIP and control IPs were loaded onto 10% SDS polyacrylamide gels and separation allowed to proceed until the dye front had moved 1cm into the separating gel. Each gel lane was then excised and subjected to in-gel digestion and liquid chromatography mass spectrometry (LC-MS) as described below.

Mass spectrometry of isolated 'pMYLK' band and SIP IPs

The gel slices were subjected to in-gel tryptic digestion using a DigestPro automated digestion unit (Intavis Ltd, Nottingham, UK). The resulting peptides were fractionated using an Ultimate 3000 nanoHPLC system (Thermo Scientific, Loughborough, UK). In brief, peptides in 1% (v/v) formic acid were injected onto an Acclaim PepMap C18 nano-trap column (Thermo Scientific). After washing with 0.5% (v/v) acetonitrile/0.1% (v/v) formic acid, peptides were resolved on a 250 mm × 75 µm Acclaim PepMap C18 reverse phase analytical column (Thermo Scientific) over a 150 min

organic gradient with a flow rate of 300 nl/min. Peptides were ionized by nano-electrospray ionization at 2.1 kV using a stainless steel emitter with an internal diameter of 30 μm (Thermo Scientific). Tandem mass spectrometry analysis (MS/MS) was carried out on a LTQ-Orbitrap Velos mass spectrometer (Thermo Scientific). The Orbitrap was set to analyse the survey scans at 60,000 resolution and the top twenty multiply charged ions in each duty cycle were selected for MS/MS in the linear ion trap. Data was acquired using the Xcalibar v2.1 software (Thermo Scientific). The raw data files from the 44-1085G IPs and the SIP IPs were processed using Proteome Discoverer software v1.2 or v1.4 respectively (Thermo Scientific) with searches performed against the UniProt Human database using the SEQUEST algorithm with the following criteria; percursor tolerance = 10 ppm, fragment tolerance = 0.8 Da, trypsin as the enzyme, carbamidomethylation of cysteine as a fixed modification and oxidation of methionine and phosphorylation of serine, threonine and tyrosine as variable modifications. The reverse database search option was enabled and all peptide data were filtered to satisfy a false discovery rate of 5%.

Knockdown of SIP with targeted siRNA.

Myometrial cells grown to 50 % confluency in 12-well plates overnight in DMEM + 10 % FCS (no penicillin or streptomycin) were incubated in the presence of 25 nM siRNA:SIP1, 5'-GACUGUCCUUCAGCUCUUC-3'; SIP2, 5'-CGTCCATATGGTGAAGAAG-3', a combination of both SIPs or non-targeting (SCR) and 3 % (v/v) Dharmafect 1 reagent for 72 hours. Cells were stimulated and lysed as above and protein knockdown verified by immunoblotting for SIP. Alternatively cells were grown for isolation of mRNA as described below.

mRNA isolation and quantitative PCR analysis.

RNA was isolated using an RNeasy mini kit (QIAGEN, West Sussex, UK) according to the manufacturer's protocol; cells were lysed in RTL buffer containing 1 % β-mercaptoethanol. Quantity and quality of RNA was assessed by the NanoDrop 1000 full spectrum 220/750-nm spectrophotometer (Labtech International, East Sussex, UK). cDNA was synthesized from 1 μg RNA using the High Capacity cDNA Reverse Transcription Kit (Applied Biosystems, Life Technologies,

Paisley, UK) following the manufacturer's instructions and diluted 5-fold on reaction completion. Gene expression was quantified by real-time quantitative PCR (RT-qPCR) with Power SYBR Green Master Mix (Applied Biosystems, Life Technologies, Paisley, UK), using a 7500 real-time PCR system (Applied Biosystems, Life Technologies, Paisley, UK). A template of 2 µl cDNA was run per reaction in a final reaction volume of 20 µl (75 nM each forward and reverse primer, Table I) for 45 cycles of 95 ˚C for 15 sec and 60 ˚C for 60 sec. A dissociation stage followed to ensure the amplification of a single product. Relative mRNA expression levels were quantified by the Pfaffl method of relative quantification (Pfaffl, 2001) and standardized to 18S (*RNA18S5*) and RNA polymerase II (*POLR2A*) levels. Expression levels were normalized to control values (SCR, non-stimulated) for graphical representation and statistical analysis.

SDS-PAGE, immunoblotting and quantification of immuno bands.

Cell or tissue lysates (15 µg or 50 µg protein, respectively) were resolved using 7.5 % Bis-Tris gels (357 mM Bis-Tris pH 6.75, 8.5 % acrylamide, 0.23 % bis-acrylamide) and MOPS running buffer (250 mM MOPS, 250 mM Tris, 5 mM EDTA, 0.5 % SDS). Proteins were transferred to polyvinylidene diflouride membrane (GE Healthcare, Buckinghamshire, UK) by wet transfer at 250 mA for 1 hour in a buffer containing 25 mM Tris, 192 mM glycine, 10 % methanol and 0.01 % SDS. Membranes were blocked in 5 % bovine serum albumin (BSA) in Tris-buffered saline + 0.1% Tween-20 (TBS-T), before incubation with primary antibodies (1 µg/ml in 5 % BSA/TBS-T) overnight at 4 °C. After washing 6 x 5 minutes in TBS-T, membranes were incubated with a horseradish peroxidase (HRP)-conjugated goat anti-rabbit antibody (#7074, 1:5000; New England Biolabs, Hitchin, UK) in TBS-T for 1 hour at room temperature. Membranes were washed for a further 6 x 5 minutes and bands visualised using an enhanced chemiluminescence system (GE Healthcare, Buckinghamshire, UK). Membranes were probed initially with phospho-specific antibodies and re-probed with the equivalent total antibody after incubating for 3 x 1 hour in stripping buffer (20 mM glycine, 1 % SDS, pH 2). Bands were quantified by densitometry using Quantity One software (Bio-Rad, Hemel Hempstead, UK), and care was taken to avoid saturation of signals. Raw data were normalised using an

experimental control for each experiment as detailed in individual figure legends, and the level of phosphorylation was always normalised using the level of equivalent total protein.

Measurement of PG release.

Primary myometrial cells were transfected with siRNA and switched to phenol red-free and serum-free medium for a total of 24 h, with EGF stimulation for 4, 8 or 24 h. Media was collected and stored at -80 °C until use. PGs were measured using the PGE metabolite enzyme-linked immunosorbent assay (ELISA) kit and the $PGF_{2\alpha}$ ELISA kit (Cayman Chemicals, MI, USA) using non-diluted media according to manufacturers' instructions.

Stimulation of myometrial explant tissue.

Freshly obtained myometrium was rinsed in sterile PBS under laminar flow and dissected into small pieces (2 mm x 2 mm) within a 100 mm tissue culture dish using a sterile scalpel. Four pieces were placed in each well of a 12-well tissue culture plate and incubated in phenol red-free DMEM + 0.5 % FCS for 4 hours. Media was replaced and explants were pre-incubated with PD-184352 (10 μM) or 0.1 % dimethylsulphoxide vehicle for 30 minutes followed by stimulation with 50 ng/ml EGF for 15 minutes or 24 hours. Individual explants were rinsed in cold PBS following stimulation, snap frozen in liquid nitrogen, and stored at -80 °C before homogenisation.

Tissue homogenisation.

For SDS-PAGE, frozen tissue explants were homogenised in SDS buffer (25 mM Tris pH 6.8, 2 % SDS, 10 % glycerol) at approximately 100mg wet weight/ml using a Polytron homogeniser at 20 °C. Lysates were immediately heated to 95 °C for 5 minutes, and cleared by centrifugation at 16,000 g for 10 minutes at 20 °C. Protein concentration was determined using the BCA assay kit (Perbio Science UK, Cramlington, UK) before 12.5 mM DTT and 0.002 % bromophenol blue were added prior to electrophoresis.

TF activation array.

The Signosis TF activation profiling array I (Stratech, Newmarket, UK) was used to determine the activity of 48 TFs following the manufacturer's instructions. Briefly, nuclear extracts from myometrial cells grown in 6 cm dishes were produced using the Nuclear Extraction Kit from Signosis. Nuclear protein (10 µg) was combined with biotin-labelled probes based on the consensus DNA binding sites for 48 TFs. After column purification, bound probes were hybridised to a 96-well plate, each well specifically pre-coated with a complementary sequence to a specific probe. After washing and incubation with strepdavidin-HRP, luminescence was measured 10 min after substrate addition for a duration of 1 s.

Statistical analyses.

Data were analysed using GraphPad Prism, version 4.3 (GraphPad, San Diego, CA, USA). The comparisons between SIP expression in uterine tissues and pregnancy were performed using one-way analysis of variance (ANOVA) with Bonferroni post hoc tests. To verify siRNA-mediated knockdown of SIP mRNA and protein, paired Student's T tests were performed. The effects of EGF-stimulation with SIP siRNA or PD-184352 treatment on COX2, IL6 and IL8 expression and phosphorylation of SIP were determined using two-way ANOVA and Bonferroni post-hoc tests. The effect of SIP siRNA on the time course of EGF-mediated PG release was determined by two-way ANOVA with repeated measures. Time course and dose-response data for SIP phosphorylation were analysed using repeated-measures ANOVA and Dunnett's post-hoc tests. Individual TF activities in SIP knockdown cells were analysed using one sample t tests against a constant of 1. A P-value of < 0.05 was considered significant for all analyses.

Results

Antibody 44-1085G detects phospho-SIP in human myometrial cells.

We used a commercially available antibody raised against phosphorylated MYLK to study MYLK phosphorylation under the influence of cyclic AMP as part of our studies on the regulation of

myometrial contractility. Using non-stimulated and FSK-treated myometrial whole cell lysates, this antibody (44-1085G) detected several bands by immunoblotting; the most reproducible and strong band was seen at approximately 100 kDa after FSK treatment (band 3, Supplementary Figure 1A). Additional bands could be seen at > 250 kDa in FSK-treated cell lysates (band 1) and at 145 kDa in both non-stimulated and stimulated conditions (band 2). Immunoblots re-probed with a MYLK antibody showed expression of the 210 kD and 110 kDa MYLK isoforms as expected (bands 4 and 5 respectively, Supplementary Figure 1B), however these did not correspond to any of the bands on the 44-1085G blot. The main 'pMYLK' band seen consistently in FSK-treated cell lysates (~ 100 kDa) was smaller than MYLK, and could easily be separated from the MYLK band using 7.5% acrylamide gels. We carried out immunoprecipitation using the 44-1085G antibody, and demonstrated by immunoblotting that MYLK was absent from these IPs; we had isolated the 100 kDa band independently of MYLK (Supplementary Figure 1A and B). To isolate this protein we cut a gel slice corresponding to the 100 kDa band by aligning the pMYLK blot with an equivalent picking gel (Supplementary Figure 1C). Tandem MS analysis of this band revealed it to be SIP (or KANK2), and several phosphorylation sites were identified in the FSK-treated IPs (Supplementary Tables I and II).

Verification of SIP phosphorylation in human myometrial cells.

A commercially available SIP antibody was used to verify the presence of SIP protein in primary myometrial cells by immunoblotting, and we were able to successfully reduce the expression of SIP protein using siRNA (Figure 1, top panel). A band of approximately 100 kDa detected using the 44-1085G antibody was increased by EGF and FSK but not by OXT or carbachol (Figure 1). The increase in response to EGF and FSK was decreased after reduction of SIP protein levels by siRNA. Moreover, the ~100 kDa band on the 44-1085G blot and the SIP band overlaid exactly. To study EGF-induced phosphorylation of SIP, the SIP antibody was used for immunoprecipitation using non- and EGF-stimulated cell lysates. Whole IPs were subjected to tandem MS and two SIP phospho-peptides were identified in EGF-stimulated IPs which were absent in non-stimulated IPs (Supplementary table III), which correspond to serine 323 and serine 375 of SIP. Taken together, our data show that the ~100 kDa band detected by antibody 44-1085G is actually SIP (in spite of the fact

that it is marketed for detection of pMYLK), EGF stimulation increases immunoreactivity of this band and concomitantly increases phosphorylation of SIP at two sites, suggesting this antibody is detecting phosphorylated SIP. The ~100 kDa band will be referred to as pSIP from this point on.

SIP is expressed in fresh human myometrium and fetal membranes.

After identification of SIP as a phospho-protein in cultured myometrial cells, the expression of SIP in fresh myometrium was verified and compared to the levels in other uterine tissues from TNIL women. SIP was detected by immunoblotting and expression was high in myometrium and in fetal membranes (combined amnion, chorion and decidua parietalis), but low in placenta and decidua basalis (Figure 2). SIP expression was subsequently studied in NP myometrium and compared to pregnant myometrium from TNIL and PNIL groups. Tissue from IOL women was also compared. SIP protein expression was significantly downregulated in pregnancy ($P < 0.05$), while there was no difference among the PNIL, TNIL and IOL groups (Figure 3).

SIP removal inhibits expression of the COX-2 gene.

SIP is involved in regulating steroid hormone-dependent transcription in a breast cancer cell line (Zhang *et al.*, 2007) and we screened several potential estrogen- or progesterone-regulated myometrial genes and steroid receptor coactivators for changes in expression in SIP siRNA-treated human myometrial cells. Knockdown of *SIP* mRNA by 71.9 ± 4.8 % (mean ± SEM; $P < 0.01$, n= 3) was associated with a decrease in the expression of *COX2* mRNA (by 34.7 ± 7.8 %, data not shown) with no appreciable effect on another 10 genes studied (*PGR*, progesterone receptor*; ESR2*, estrogen receptor 2; *OXTR*, oxytocin receptor; *COX1*, prostaglandin-endoperoxide synthase 1*; PTGFR*, prostaglandin F receptor; *PTGER2*, prostaglandin E receptor 2*; PTGER3*, prostaglandin E receptor 3; *PTGES*, prostaglandin E synthase; *NCOA1*, nuclear receptor coactivator 1 and *NCOA2*, nuclear receptor coactivator 2; data not shown).

SIP is involved in EGF-stimulated expression of COX2 mRNA and protein.

EGF strongly stimulates COX2 expression in primary human amnion (Zakar *et al.* , 1998) and myometrial cells (Wouters *et al.*, 2014) leading us to investigate the role of SIP in this effect. In our study, exposure of myometrial cells to two individual SIP siRNAs in combination resulted in a decrease in *SIP* mRNA expression (Figure 4A). Treatment with EGF for 24 h resulted in a significant increase in *COX2* mRNA (2.47 ± 0.52 fold, $P < 0.05$) and this effect was impaired in siRNA-treated cells (Figure 4B). Treatment of myometrial cells with two individual SIP siRNAs separately and in combination resulted in a large decrease in SIP protein expression (Figure 4C and D). COX2 protein expression was significantly increased after 24 h EGF stimulation (3.86 ± 0.49 fold, $P < 0.001$, Figure 4C and E), while EGF was unable to significantly increase COX2 expression in cells with SIP knockdown. The level of EGF-stimulated COX2 protein was also significantly decreased in SIP knockdown cells when compared to scrambled controls (0.86 ± 0.47 versus 3.86 ± 0.49 fold, $P < 0.001$, Figure 4E). The mRNA and protein data taken together suggest a role for SIP in EGF-mediated expression of the *COX*2.

EGF-stimulated increases in PGE_2 and $PGF_{2\alpha}$ production are SIP-dependent.

To further investigate the role of SIP in PG synthesis, PGE_2 and $PGF_{2\alpha}$ release were measured after EGF treatment and SIP knockdown. EGF was able to stimulate release of PGE_2 from primary myometrial cells after 8 h, and these effects were blocked in cells with SIP knockdown *($P < 0.001$*, Figure 5A). Modest but significant increases in $PGF_{2\alpha}$ output were measured after 24 h EGF treatment, and similarly these were reduced after SIP knockdown ($P < 0.01$, Figure 5B).

The ERK1/2 signalling pathway is required for both EGF-stimulated SIP phosphorylation and EGF-induced COX2 expression.

EGF treatment caused phosphorylation of SIP in a dose-dependent manner; significant phosphorylation was detected as low as 1 ng/ml EGF with maximal phosphorylation achieved between 10 and 25 ng/ml EGF, and phosphorylation decreasing again with 100 ng/ml EGF (Figure

6A and B). EGF-induced phosphorylation of SIP was transient; significant increases were detected between 5 and 30 minutes, with maximal phosphorylation at the 15 minute time point and de-phosphorylation occurring by 60 minutes (Figure 6C and D). EGF stimulation resulted in dose- and time-dependent phosphorylation of ERK1/2 within its activation loop (Figure 6A and C). Since ERK1/2 is known to play a role in EGF-stimulated COX2 expression (Molnar *et al.*, 1999, Wouters *et al.*, 2014), its involvement in SIP phosphorylation was investigated. EGF stimulation resulted in concomitant phosphorylation of both SIP and ERK1/2, and SIP knockdown did not affect EGF-stimulated ERK1/2 phosphorylation (Figure 7A, B and C). The MEK1 inhibitor PD-184352 ablated ERK phosphorylation in both stimulated and non-stimulated cells (Figure 7C). PD-184352 significantly reduced the level of SIP phosphorylation in EGF-treated cells by 81.5 ± 2.50 % ($P < 0.001$, n=5, Figure 7B). Additionally, EGF was no longer able to stimulate expression of COX2 in PD-184352 treated cells (Figure 7D and E) confirming our previous data (Wouters *et al.*, 2014). Taken together these results suggest that ERK lies upstream of SIP phosphorylation and both ERK and SIP contribute to EGF-induced COX2 expression.

EGF-induced SIP phosphorylation and COX2 induction in fresh human myometrial tissue.

The phosphorylation of SIP in freshly isolated myometrium was investigated alongside EGF-stimulated changes in COX2 expression. EGF was able to significantly stimulate SIP phosphorylation in myometrial explants (1.94 fold ± 0.26, $P < 0.01$) which was reduced in cells pre-incubated with the MEK1 inhibitor PD-184352 (1.94 fold ± 0.26 versus 0.68 fold ± 0.21, $P < 0.01$, Figure 8A). Treatment of myometrial tissue with EGF for 24 hours resulted in enhanced protein expression of COX2 ($P < 0.05$ for overall effect of EGF), with some effect of MEK1 inhibition ($P = 0.053$ for overall effect of PD-184352).

SIP in involved in regulating production of pro-inflammatory cytokines.

Since COX2 is up-regulated during labour in human myometrium, we expanded our studies on SIP function to measure the expression of some pro-inflammatory cytokines and chemokines implicated

in the initiation of labour. Very low levels of *IL1B* mRNA in primary myometrial cells were detected relative to *IL6, IL8 (CXCL8)* and *TNF* mRNAs (Figure 9A). *IL6* and *IL8* mRNAs were increased in response to EGF treatment (1.81 ± 0.35 fold and 2.97 ± 0.88 fold respectively), with SIP knockdown causing an overall decrease in expression of *IL6* and *IL8,* which was statistically significant (Figures 9C and D, $P < 0.05$). Despite very low levels of *IL1B* mRNA, EGF caused modest increases which were SIP dependent (Figure 9B), while there was no significant effect of EGF or SIP knockdown on *TNF* mRNA expression (Figure E).

SIP is involved in negatively regulating the activity of multiple TFs.

To test the hypothesis that SIP mediates its effects on *COX2, IL6* and *IL8* expression by modulating TF activity, we carried out a profile of TF activation in SIP knockdown cells relative to cells transfected with scrambled siRNA. A total of 47 TFs were assessed by their ability to bind their consensus DNA sequences using a commercially available array. The effect of SIP knockdown on TF activity ranged from a mean ± SEM of 0.63 ± 0.18 to 14.47 ± 3.96 fold (n=3, Supplementary Table IV), however there were considerable variations in TF activity between the three experiments conducted. TFs with the greatest change in activity after SIP knockdown are shown in Figure 10; reduction in SIP expression resulted in increased activity of serum response factor (SRF), signal transducer and activator of transcription (STAT) 2, YY1 TF (YY1), SMAD family (SMAD), nuclear receptor subfamily 1 group I member 3 (NR1I3**)**, glucocorticoid receptor/progesterone receptor (GR/PR), NFKB1, STAT5, CCAAT/enhancer binding protein zeta (CEBPZ); and early growth response (EGR), although only two of these were statistically significant. Large and significant increases in SRF (14.47 ± 3.96 fold, $P < 0.001$) and YY1 (12.84 ± 6.37, $P < 0.05$) with SIP knockdown suggest that SIP functions to negatively regulate the activity of these TFs in human myometrial cells.

Discussion

This is the first description of SIP expression and function in uterine tissues. SIP was identified in FSK-stimulated human myometrial cell lysates by MS. The expression of SIP protein was high in myometrium and amnion/chorion/decidua (parietalis) but low in placenta and decidua basalis. EGF caused ERK-dependent phosphorylation of SIP in myometrial cells at a site, or sites, detectable using antibody 44-1085G which is actually marketed for detection of pMYLK. This antibody, in combination with siRNA knockdown of SIP as a negative control, has proved a valuable tool for measuring SIP phosphorylation. Targeted siRNA knockdown of SIP has also revealed that SIP is required for EGF-stimulated COX2 expression and resulting PG release, in addition to expression of *IL6* and *IL8* mRNAs in human myometrium.

SIP binds to the steroid receptor co-activator protein SRC-1 (NCOA1), thereby sequestering SRC-1 in the cytoplasm and negatively regulating estrogen-dependent transcription in a breast cancer cell line (Zhang *et al.*, 2007), however there is no published information about the functional roles of SIP in uterine tissues. We screened genes that are potentially regulated by steroid hormones, and the steroid receptor coactivators, *SRC1 (NCOA1)* and *SRC2 (NCOA2)* in myometrium. This revealed that SIP removal decreases expression of *COX2* mRNA. Myometrial COX2 expression can be stimulated by a variety of pro-inflammatory cytokines, and by OXT, PGs and EGF (Chen *et al.*, 2012, Molnar *et al.*, 1999, Phillips *et al.*, 2011, Sooranna *et al.*, 2004, Wouters *et al.*, 2014), and since EGF was capable of phosphorylating SIP we focussed on determining the role of SIP in EGF-induced myometrial COX2 expression. SIP depletion by siRNA decreased the ability of EGF to stimulate *COX2* mRNA and COX2 protein expression. Importantly, reduction of SIP also inhibited PGE_2 and $PGF_{2\alpha}$ production in response to EGF. To investigate the signalling pathways upstream of SIP, pharmacological inhibition of MEK1/ERK signalling was achieved with PD-184352. ERK1/2 activity was required both for the phosphorylation of SIP and up-regulation of COX2 protein expression in response to EGF. Moreover, SIP knockdown did not affect the ability of EGF to activate ERK1/2, placing SIP downstream of ERK1/2 activation and upstream of COX2 regulation. The data replicate previous observations that EGF-mediated COX2 expression requires ERK1/2 signalling (Wouters *et al.*, 2014), and demonstrate

the functional involvement of SIP in this pathway. No effect of SIP knockdown on pro-inflammatory cytokine (IL1B)-induced COX2 expression was observed (data not shown) however since the magnitude of IL1B-induced COX2 is so large, alternative pathways such as NFKB may dominate over SIP involvement (Wouters *et al.*, 2014). Since uterine COX2 is a key regulator of PG synthesis at labour, we expanded our study on SIP to investigate its regulation of other pro-labour mediators. SIP was positively involved in EGF-stimulated myometrial *IL6* and *IL8* mRNA expression, which have both been shown to increase with labour (Osmers *et al.*, 1995, Tattersall *et al.*, 2008). Taken together, these data support our hypothesis that SIP plays a role in regulating labour-related gene expression in human myometrium. While no difference in SIP protein expression was seen between non-labouring myometrium and that taken after labour induction, this does not exclude the possibility of transient changes in SIP expression at the onset of spontaneous labour. Moreover, the functional significance of the relatively high level of SIP expression in amnion/chorio-decidua in pregnancy needs to be investigated.

Further investigations into the mechanism of action for SIP led us to demonstrate that SIP expression is negatively associated with the activity of several TFs, in particular SRF and YY1. SRF and YY1 can both bind to the serum response element (SRE) and the observation that YY1 enhances binding of SRF to SRE (Natesan *et al.*, 1995) highlights a relevant pathway that is potentially regulated by SIP. Since ERK signalling results in phosphorylation of SIP and also phosphorylation of SRF (Rivera *et al.*, 1993) the functional interaction between SIP and SRF is likely to be a fruitful area of research. It is possible that SIP may positively or negatively affect TF activity by binding and sequestering either co-repressors or co-activators in the cytoplasm (Ramot *et al.* , 2014, Zhang *et al.* , 2007), although the identity of such factors remains to be determined.

Two sites of SIP phosphorylation detectable only after EGF stimulation have been identified during MS experiments, namely serine 323 and serine 375. Serine 323 lies within a medium stringency consensus motif for both cyclin-dependent kinase (CDK) 1 and CDK5 phosphorylation. Serine 375 lies within a medium stringency consensus motif for ERK1, glycogen synthase kinase 3, CDK1 and

CDK5 phosphorylation, and a low stringency consensus motif for 14-3-3 zeta/delta binding (Obenauer *et al.* , 2003). We propose that phosphorylation of SIP is required for its role as a transcriptional regulator, and identification of these sites suggests that ERK1/2 may directly phosphorylate SIP at serine 375. However more studies are required to verify the specific sites of phosphorylation, the protein kinases involved and their functional significance.

EGF is released by the fetus into the amniotic fluid during pregnancy and levels increase rapidly in late pregnancy (Hofmann and Abramowicz, 1990, Varner *et al.* , 1996). While some studies have demonstrated no effect of labour on amniotic EGF levels (Hofmann and Abramowicz, 1990), others have shown that EGF increases with labour (Romero *et al.* , 1989) and in cases of premature rupture of the membranes with and without underlying infection (Shobokshi and Shaarawy, 2002). EGF exerts its function by binding to the EGF receptor (EGFR, the first described member of the ErbB tyrosine kinase family). EGF and EGFR mRNAs have both been detected in human myometrial cells (Yeh *et al.* , 1991). Binding of EGF to EGFR stimulates its tyrosine kinase activity leading to EGFR auto-phosphorylation (Honegger *et al.* , 1990), resulting in recruitment of adaptor proteins and activation of signalling pathways such as ERK1/2, phospholipase C gamma, PKC, phosphatidylinositol 3-kinase - Akt and NFKB (Jorissen *et al.* , 2003). In parallel to amniotic fluid EGF levels, COX2 in fetal membranes increases during gestation and further with labour (Slater *et al.*, 1999a), and in myometrium with labour at term and preterm (Slater *et al.*, 1999b). The subsequent intra-uterine release of PGs facilitates labour by coordinating membrane rupture, myometrial contractions and cervical ripening. It is tempting to speculate that EGF-mediated increases in COX2 and PG release could be important during the initiation of labour, particularly in a supporting role to the action of OXT or inflammatory cytokines.

In summary, we have found that an antibody marketed for detection of pMYLK actually provides a unique tool for detection of pSIP. Exploiting this serendipitous observation we have made several novel findings pertinent to myometrial cell signalling (Figure 11): a) that SIP is expressed in human myometrium and fetal membranes, b) that EGF causes ERK-dependent phosphorylation of SIP, c)

that ERK and SIP are involved in EGF-stimulated COX2 expression, and d) that SIP regulates EGF-dependent release of PGs. We suggest that SIP may be directly phosphorylated and regulated by ERK and propose that SIP regulates the activity of multiple TFs, providing novel mechanisms for modifying gene expression. These findings increase our understanding of the complex mechanisms regulating the transition into human labour involving increased PG production, and could lead to the development of new, targeted drugs for the control of uterine activation in the management of preterm labour.

Acknowledgments

We are grateful for the help of research midwife Emily Bradley-Smith for obtaining informed consent from women at St Michael's hospital, Bristol, and collecting samples of uterine tissue. We also thank Dr Gavin Welsh, University of Bristol, for helpful discussions and Dr Kate Heesom, University of Bristol Proteomics facility, for mass spectrometry analysis.

Authors' Roles

C.A.H contributed to study design and conducted all experiments, analysed and interpreted the data, and wrote the manuscript. C.A.M. contributed to data interpretation and manuscript revision, A.L.B. contributed to study design, data interpretation and manuscript revision.

Funding

This work was funded by an Action Medical Research grant, number SP4612.

Conflict of Interest

The authors have no competing interests to declare.

References

Ackerman WEt, Rovin BH, Kniss DA. Epidermal growth factor and interleukin-1beta utilize divergent signaling pathways to synergistically upregulate cyclooxygenase-2 gene expression in human amnion-derived WISH cells. *Biol Reprod*. 2004*;* **71**: 2079-86.

Chen L, Sooranna SR, Lei K, Kandola M, Bennett PR, Liang Z, Grammatopoulos D, Johnson MR. Cyclic AMP increases COX-2 expression via mitogen-activated kinase in human myometrial cells. *Journal of Cellular and Molecular Medicine*. 2012*;* **16**: 1447-60.

Erkinheimo TL, Saukkonen K, Narko K, Jalkanen J, Ylikorkala O, Ristimaki A. Expression of cyclooxygenase-2 and prostanoid receptors by human myometrium. *J Clin Endocrinol Metab*. 2000*;* **85**: 3468-75.

Gee HY, Zhang F, Ashraf S, Kohl S, Sadowski CE, Vega-Warner V, Zhou W, Lovric S, Fang H, Nettleton M *et al.* KANK deficiency leads to podocyte dysfunction and nephrotic syndrome. *J Clin Invest*. 2015; **125**: 2375-84.

Haas DM, Caldwell DM, Kirkpatrick P, McIntosh JJ, Welton NJ. Tocolytic therapy for preterm delivery: systematic review and network meta-analysis. *BMJ*. 2012*;* **345**.

Hofmann GE, Abramowicz JS. Epidermal Growth Factor (Egf) Concentrations in Amniotic Fluid and Maternal Urine During Pregnancy. *Acta Obstetricia et Gynecologica Scandinavica*. 1990*;* **69**: 217-21.

Honegger AM, Schmidt A, Ullrich A, Schlessinger J. Evidence for epidermal growth factor (EGF)-induced intermolecular autophosphorylation of the EGF receptors in living cells. *Mol Cell Biol*. 1990*;* **10**: 4035-44.

Jorissen RN, Walker F, Pouliot N, Garrett TPJ, Ward CW, Burgess AW. Epidermal growth factor receptor: mechanisms of activation and signalling. *Experimental Cell Research*. 2003*;* **284**: 31-53.

Kakinuma N, Roy BC, Zhu Y, Wang Y, Kiyama R. Kank regulates RhoA-dependent formation of actin stress fibers and cell migration via 14-3-3 in PI3K-Akt signaling. *J Cell Biol*. 2008*;* **181**: 537-49.

Kakinuma N, Zhu Y, Wang Y, Roy BC, Kiyama R. Kank proteins: structure, functions and diseases. *Cell Mol Life Sci*. 2009*;* **66**: 2651-9.

596 Kaminski K, Rechberger T, Oleszczuk J, Jakowicki J, Oleszczuk J. Biochemical and clinical
597 evaluation of the efficiency of intracervical extraamniotic prostaglandin F2 alpha and intravenous
598 oxytocin infusion to induce labour at term. *The Australian & New Zealand journal of obstetrics &*
599 *gynaecology*. 1994*;* **34**: 409-13.
600 Kang YJ, Mbonye UR, DeLong CJ, Wada M, Smith WL. Regulation of intracellular cyclooxygenase
601 levels by gene transcription and protein degradation. *Progress in lipid research*. 2007*;* **46**: 108-25.
602 Keirse MJ. Biosynthesis and metabolism of prostaglandins in the pregnant human uterus. *Advances in*
603 *prostaglandin and thromboxane research*. 1978*;* **4**: 87-102.
604 Lee SE, Park IS, Romero R, Yoon BH. Amniotic fluid prostaglandin F2 increases even in sterile
605 amniotic fluid and is an independent predictor of impending delivery in preterm premature rupture of
606 membranes. *The Journal of Maternal-Fetal & Neonatal Medicine*. 2009*;* **22**: 880-6.
607 Lopez Bernal A, Hansell DJ, Khong TY, Keeling JW, Turnbull AC. Prostaglandin E production by
608 the fetal membranes in unexplained preterm labour and preterm labour associated with
609 chorioamnionitis. *Br J Obstet Gynaecol*. 1989*;* **96**: 1133-9.
610 Mohan AR, Sooranna SR, Lindstrom TM, Johnson MR, Bennett PR. The effect of mechanical stretch
611 on cyclooxygenase type 2 expression and activator protein-1 and nuclear factor-κB activity in human
612 amnion cells. *Endocrinology*. 2007*;* **148**: 1850-7.
613 Molnar M, Rigo J, Jr., Romero R, Hertelendy F. Oxytocin activates mitogen-activated protein kinase
614 and up-regulates cyclooxygenase-2 and prostaglandin production in human myometrial cells. *Am J*
615 *Obstet Gynecol*. 1999*;* **181**: 42-9.
616 Natesan S, Gilman M. YY1 facilitates the association of serum response factor with the c-fos serum
617 response element. *Molecular and Cellular Biology*. 1995; **15**: 5975-82.
618 Obenauer JC, Cantley LC, Yaffe MB. Scansite 2.0: Proteome-wide prediction of cell signaling
619 interactions using short sequence motifs. *Nucleic acids research*. 2003*;* **31**: 3635-41.
620 Osmers RGW, BlÃ SJ, Kuhn W, Tschesche H. Interleukin-8 Synthesis and the Onset of Labor.
621 *Obstetrics & Gynecology*. 1995 ; **86**: 223-9.
622 Pfaffl MW. A new mathematical model for relative quantification in real-time RT-PCR. *Nucleic acids*
623 *research*. 2001*;* **29**: e45.

624 Phillips RJ, Al-Zamil H, Hunt LP, Fortier MA, López Bernal A. Genes for prostaglandin synthesis,
625 transport and inactivation are differentially expressed in human uterine tissues, and the prostaglandin
626 F synthase AKR1B1 is induced in myometrial cells by inflammatory cytokines. *Molecular Human*
627 *Reproduction*. 2011*;* **17**: 1-13.
628 Phillips RJ, Fortier MA, López Bernal A. Prostaglandin pathway gene expression in human placenta,
629 amnion and choriodecidua is differentially affected by preterm and term labour and by uterine
630 inflammation. *BMC Pregnancy and Childbirth*. 2014*;* **14**: 241.
631 Pont JNA, McArdle CA, López Bernal A. Oxytocin-Stimulated NFAT Transcriptional Activation in
632 Human Myometrial Cells. *Molecular Endocrinology*. 2012; **17**: 1743-56.
633 Ramot Y, Molho-Pessach V, Meir T, Alper-Pinus R, Siam I, Tams S, Babay S, Zlotogorski A.
634 Mutation in KANK2, encoding a sequestering protein for steroid receptor coactivators, causes
635 keratoderma and woolly hair. *Journal of medical genetics.* 2014; **51**: 388-94.
636 Rivera VM, Miranti CK, Misra RP, Ginty DD, Chen RH, Blenis J, Greenberg ME. A growth factor-
637 induced kinase phosphorylates the serum response factor at a site that regulates its DNA-binding
638 activity. *Molecular and Cellular Biology.* 1993; **13**: 6260-73.
639 Romero R, Emamian M, Wan M, Quintero R, Hobbins JC, Mitchell MD. Prostaglandin
640 concentrations in amniotic fluid of women with intra-amniotic infection and preterm labor. *American*
641 *Journal of Obstetrics and Gynecology*. 1987*;* **157**: 1461-7.
642 Romero R, Wu YK, Oyarzun E, Hobbins JC, Mitchell MD. A potential role for epidermal growth
643 factor/alpha-transforming growth factor in human parturition. *Eur J Obstet Gynecol Reprod Biol*.
644 1989*;* **33**: 55-60.
645 Sellers SM, Hodgson HT, Mitchell MD, Anderson AB, Turnbull AC. Raised prostaglandin levels in
646 the third stage of labor. *Am J Obstet Gynecol*. 1982*;* **144**: 209-12.
647 Shobokshi A, Shaarawy M. Maternal serum and amniotic fluid cytokines in patients with preterm
648 premature rupture of membranes with and without intrauterine infection. *International Journal of*
649 *Gynecology & Obstetrics*. 2002*;* **79**: 209-15.

650 Slater D, Dennes W, Sawdy R, Allport V, Bennett P. Expression of cyclo-oxygenase types-1 and -2 in
651 human fetal membranes throughout pregnancy. *Journal of Molecular Endocrinology*. 1999a*;* **22**: 125-
652 30.
653 Slater DM, Dennes WJB, Campa JS, Poston L, Bennett PR. Expression of cyclo-oxygenase types-1
654 and -2 in human myometrium throughout pregnancy. *Molecular Human Reproduction*. 1999b*;* **5**: 880-
655 4.
656 Sooranna SR, Lee Y, Kim LU, Mohan AR, Bennett PR, Johnson MR. Mechanical stretch activates
657 type 2 cyclooxygenase via activator protein-1 transcription factor in human myometrial cells.
658 *Molecular Human Reproduction*. 2004*;* **10**: 109-13.
659 Tattersall M, Engineer N, Khanjani S, Sooranna SR, Roberts VH, Grigsby PL, Liang Z, Myatt L,
660 Johnson MR. Pro-labour myometrial gene expression: are preterm labour and term labour the same?
661 *Reproduction.* 2008; **135**: 569-79.
662 Varner MW, Dildy GA, Hunter C, Dudley DJ, Clark SL, Mitchell MD. Amniotic Fluid Epidermal
663 Growth Factor Levels in Normal and Abnormal Pregnancies. *Journal of the Society for Gynecologic*
664 *Investigation*. 1996*;* **3**: 17-9.
665 Wang D, Liang J, Zhang Y, Gui B, Wang F, Yi X, Sun L, Yao Z, Shang Y. Steroid receptor
666 coactivator-interacting protein (SIP) inhibits caspase-independent apoptosis by preventing apoptosis-
667 inducing factor (AIF) from being released from mitochondria. *J Biol Chem*. 2012*;* **287**: 12612-21.
668 Wouters E, Hudson CA, McArdle CA, López Bernal A. Central role for protein kinase C in oxytocin
669 and epidermal growth factor stimulated cyclooxygenase 2 expression in human myometrial cells.
670 *BMC Research Notes*. 2014*;* **7**: 357.
671 Yeh J, Rein M, Nowak R. Presence of messenger ribonucleic acid for epidermal growth factor (EGF)
672 and EGF receptor demonstrable in monolayer cell cultures of myometria and leiomyomata. *Fertil*
673 *Steril*. 1991*;* **56**: 997-1000.
674 Zakar T, Mijovic JE, Eyster KM, Bhardwaj D, Olson DM. Regulation of prostaglandin H2 synthase-2
675 expression in primary human amnion cells by tyrosine kinase dependent mechanisms. *Biochim*
676 *Biophys Acta*. 1998*;* **1391**: 37-51.

677 Zhang Y, Zhang H, Liang J, Yu W, Shang Y. SIP, a novel ankyrin repeat containing protein,
678 sequesters steroid receptor coactivators in the cytoplasm. *The EMBO Journal*. 2007*;* **26**: 2645-57.
679 Zhu Y, Kakinuma N, Wang Y, Kiyama R. Kank proteins: a new family of ankyrin-repeat domain-
680 containing proteins. *Biochim Biophys Acta*. 2008*;* **1780**: 128-33.

681

Figure 1. Steroid receptor co-activator interacting protein (SIP) is phosphorylated in human myometrial cells by epidermal growth factor (EGF) and forskolin (FSK).

Cultured myometrial cells were transfected with non-targeting siRNA (-) or siRNA targeted to SIP (+) before being stimulated with oxytocin (**OXT**; 10nM, 5 mins), **EGF** (25 ng/ml, 15 mins), carbachol (**CCh**; 200 µM, 5 mins) or **FSK** (10 µM, 15 mins). Cells lysates were resolved by SDS-PAGE and immunoblotting carried out for SIP and pSIP, the latter measured using antibody 44-1085G raised against phosphorylated myosin light chain kinase (pMYLK). The pSIP bands were reduced in SIP siRNA samples confirming their identity.

Figure 2. SIP is predominantly expressed in human amnion/chorion/decidua and myometrium, with poor expression in placenta and decidua basalis.

Tissues were collected from women not in labour undergoing caesarean section at term and snap frozen until homogenisation as per Methods. **A**, tissue homogenates were resolved by SDS-PAGE and immunoblotting was carried out for SIP and RhoGDI (loading control). **B**, SIP levels were quantified by densitometry and standardised over multiple gels using an internal control (a mixture of all tissue lysates). Data were further normalised to the level of RhoGDI. **PLA**, placenta; **DEC**, decidua basalis; **ACD**, amnion/chorion/decidua parietalis; **MYO**, myometrium. Data were analysed using one-way analysis of variance (ANOVA) and Tukey's post-hoc tests; * $P < 0.05$ for the comparisons between PLA or DEC and ACD, and ** $P < 0.01$ for the comparisons between PLA or DEC and MYO.

Figure 3. Myometrial SIP expression decreases with pregnancy and is unchanged after induction of labour.

Myometrium was collected from women undergoing non-pregnant hysterectomy (**NP**, n=4), caesarean section without labour before 37 weeks (**PNIL**, n=6) or at term (**TNIL**, n=6), and after induction of labour at term (**IOL**, n=4). Tissues were and snap frozen until homogenisation as described in Methods. **A**, tissue homogenates were resolved by SDS-PAGE and immunoblotting was carried out for SIP and RhoGDI (loading control), a representative blot is shown. Samples were from

the same gel but discontinuous lanes (horizontal line). **B**, SIP levels were quantified by densitometry and standardised over multiple gels using an internal control (a mixture of all tissue lysates). Data were further normalised to the level of RhoGDI and analysed using one-way ANOVA and Bonferroni post-hoc tests; * $P < 0.05$ for the comparisons between NP and PNIL, TNIL or IOL.

Figure 4. SIP in involved in EGF-stimulated increases in COX2 mRNA and protein.

Primary myometrial cells were transfected with scrambled siRNA (**SCR**) or siRNA targeting SIP; siRNA 1 (**SIP1**), siRNA 2 (**SIP2**) or a combination of both siRNAs (**S1/2**). Two days following transfection cells were left as non-stimulated controls (**CON**) or treated with 25 ng/ml **EGF** for 24 h. RT-qPCR for *SIP* (**A)** and *COX2* (**B)** was performed, data were normalised using ribosomal 18S (*RNA18S5*) and RNA polymerase (*POLR2A*) and then expressed as fold change relative to SCR, CON. Statistics were performed using a paired Student's T test (**A**) or 2-way ANOVA and Bonferroni post-hoc tests (**B**); $, $P < 0.001$ for knockdown of *SIP* mRNA, n=6; * $P < 0.05$ for effect of EGF in SCR, n=3; ns, not significant for effect of EGF in S1/2. **C**, immunoblotting for SIP, COX2 and glyceraldehyde-3-phosphate dehydrogenase (GAPDH) was performed and SIP knockdown in non-stimulated cells was quantified (**D**, $, $P < 0.001$**,** n=8). **C**, COX2 levels were quantified, normalised to GAPDH levels then expressed as fold change compared to SCR, CON. Statistics were performed using a paired Student's T test (**A**) or 2-way ANOVA and Bonferroni post-hoc tests (**B**); $P = 0.007$ for overall effect of SIP siRNA; $, $P < 0.001$ for effect of EGF in SCR and effect of S1/2 siRNA in EGF-stimulated cells; ns, not significant for effect of EGF with S1/2 siRNA, n = 4.

Figure 5. EGF-stimulated increases in PGE_2 and $PGF_{2\alpha}$ production are dependent on SIP.

Primary human myometrial cells were transfected with scrambled siRNA (**SCR**) or 2 separate siRNAs targeting SIP (**SIP**). Two days following transfection cells were not treated or treated with 25

ng/ml **EGF** for 4, 8 or 24 h. PGE_2 metabolites and $PGF_{2\alpha}$ were assayed in the culture media using commercially available kits as per methods. Statistics were performed using 2-way ANOVA with repeated measures and Bonferroni post-hoc tests *, $P < 0.05$, ** $P < 0.01$ and ***, $P < 0.001$ for the effect of EGF at 8 or 24 h relative to non-stimulated; [a], $P < 0.05$, [b], $P < 0.01$ and [c], $P < 0.001$ for the effect of SIP siRNA at 8 or 24 h relative to SCR.

Figure 6. EGF phosphorylates SIP in a dose- and time-dependent manner.

Primary human myometrial cells grown until confluent were serum starved for 4 hours before being treated. **A** and **B**, cells were treated with increasing concentrations of EGF as shown for 15 min. **B** and **D**, cells were treated with 25 ng/ml EGF for increasing time as shown. Immunoblotting was carried out for pSIP, SIP, pERK and ERK; pSIP was quantified by densitometry, normalised to total SIP levels and expressed as a percentage of maximal phosphorylation. Statistics were performed using repeated-measures ANOVA and Dunnett's post-hoc tests, *, $P < 0.01$ relative to non-stimulated; n = 5.

Figure 7. The ERK1 pathway is required for both EGF-stimulated SIP phosphorylation and EGF-induced COX2 expression.

A, B and **C**, primary human myometrial cells transfected with non-targeting siRNA or siRNA targeted to **SIP**. They were subsequently pre-treated with PD-184352 (**PD**; 10μM for 30 min) or vehicle control (**VEH**, 0.1% DMSO) before remaining non-stimulated (**CON**) or treated with 25 ng/ml **EGF** for 15 min. **A**, Immunoblotting for pSIP, SIP, pERK1/2 and ERK1/2 was performed. Samples were loaded on a single gel but were in discontinuous lanes (solid line) **B**, pSIP levels were quantified and normalised to the level of total SIP, and expressed as a percentage of the EGF-stimulated value. **C**, pERK1/2 levels were quantified and normalised to the levels of total ERK1/2 and expressed as a percentage of the EGF-stimulated value. Statistics were performed using 2-way ANOVA and Bonferroni post-hoc tests, $, $P < 0.001$; #, $P < 0.01$; *, $< P < 0.05$; n = 5. **D**, cells were pre-treated with or without PD-184352 as above and subsequently stimulated with or without 25

ng/ml EGF for 24 h. Immunoblotting was carried out for COX2 and GAPDH, samples were loaded on a single gel but were in discontinuous lanes (solid line) **E**, COX2 levels were quantified, normalised by levels of GAPDH and expressed as a percentage of the EGF-stimulated value. Statistics were performed using 2-way ANOVA and Bonferroni post-hoc tests; #, $P < 0.01$; NS, non-significant; n = 3.

Figure 8. EGF-induced SIP phosphorylation and COX2 expression in fresh human myometrial tissue.

Myometrial explants in culture were treated for either 15 min (**A**) or 24 h (**B**) with EGF, following pre-treatment for 30 min with PD-184352 (**PD**) or DMSO vehicle control (**VEH**). After snap freezing and homogenising the muscle, proteins were resolved by SDS-PAGE and immunoblotting carried out for pSIP, SIP, COX2 or RhoGDI (loading control). The levels of pSIP and COX2 were quantified by densitometry, normalised to the level of SIP and RhoGDI respectively, and expressed as fold change relative to CON, VEH. Statistics were performed using 2-way ANOVA and Bonferroni post hoc tests; #, $P < 0.01$; n=4 (**A**). *****, $P < 0.05$ for the overall effect of EGF, n=4 (**B**).

Figure 9. SIP is involved in regulating production of pro-inflammatory cytokines.

Relative levels of *IL1B*, *IL6*, *IL8 (CXCL8)* and *TNFα* mRNA in non-stimulated primary myometrial cells were determined by RT-pPCR (**A**). Myometrial cells were transfected with scrambled siRNA (**SCR**) or a combination of two SIP siRNAs (**SIP**). Two days following transfection cells were left as non-stimulated controls (**CON**) or treated with 25 ng/ml **EGF** for 24 h. RT-qPCR for *IL1B* (**B)**, *IL6* (**C),** *IL8 (CXCL8)* (**D)** or *TNF* (**E)** was performed, data were normalised using *RNA18S5* and *POLR2A* and then expressed as fold change relative to SCR, CON. Statistics were performed using 2-way ANOVA and Bonferroni post-hoc tests; * $P < 0.05$ and ** $P < 0.01$ for overall effect of EGF or overall effect of SIP siRNA for *IL6* and *IL8*, n=4.

Figure 10. SIP is involved in negatively regulating the activity of multiple transcription factors (TFs).

Primary human myometrial cells were transfected with scrambled siRNA (**SCR**) or a combination of two SIP siRNAs (**SIP**). The activation of 47 TFs was assayed in nuclear extracts by their ability to bind their consensus DNA sequence, using a commercially available array, as per methods. Data are presented as fold activation in **SIP** relative to **SCR** (mean ± SEM, n = 3) and the top 10 TFs with the greatest change are shown. *** $P < 0.001$ and * $P < 0.05$ using one-sample t-tests against a constant of 1. **SRF**, serum response factor; **STAT2**, signal transducer and activator of transcription 2; **YY1**, YY1 transcription factor; **SMAD**, SMAD family; **NR1I3**, Nuclear receptor subfamily 1 group I member 3; **GR/PR**, glucocorticoid receptor/progesterone receptor; **NFKB**, nuclear factor kappa B 1; **STAT5**, signal transducer and activator of transcription 5; **CEBPZ**, CCAAT/enhancer binding protein zeta; **EGR**, early growth response.

Figure 11. Summary pathways for myometrial SIP function.

Proposed pathways for EGF-mediated and SIP-dependent COX2 expression and PG release. SIP knockdown inhibits expression of COX2, IL6, IL8 and PG release. Conversely SIP knockdown causes increased activity of several TFs including SRF and YY1. Dashed lines represent additional possible pathways. Through these pathways SIP is likely to participate in the complex mechanism of human parturition.

Supplementary figure 1. Immunoprecipitation with pMYLK (44-1085G) antibody for identification of SIP.

Myometrial cells were non-stimulated (CON) or stimulated with 10 μM FSK for 15 mins and subsequently lysed as per Methods. Immunoprecipitation of both lysates was carried out using a pMYLK antibody (44-1085G); immunoprecipitates (IPs) and whole cell lysates (WCL) were run on two SDS-PAGE gels in parallel. One gel was used for immunoblotting using the 44-1085G antibody (**A**) and re-probed for MYLK (**B**) and the second was silver stained (**C**). After overlay of the 44-

1085G immunoblot (IB) and silver stained gel, a gel slice equivalent to the ~ 100 kDa 44-1085G immunogen (highlighted in a box on the 44-1085G blot and gel) was cut from the silver stained gel. Bands referred to in Results are indicated by arrows numbered 1-5.

Target	Accession #	Forward primer (5'–3')	Position	Reverse primer (5'–3')	Position
RNA18S5	NR_003286	ATGGCCGTTCTTAGTTGGTG	1332	CGCTGAGCCAGTCAGTGTAG	1548
POLR2A	NM_000937	GCACCACGTCCAATGACATTG	4453	GTGCGGCTGCTTCCATAAGC	4719
COX2	NM_000963	CAAAGGTAAAAAGCAGCTTCCT	590	CTGGGGATCAGGGATGAACT	671
SIP	NM_015493	CCCAGAAGTTCCTGCCGAAT	1333	GACTCTTGGGAGGCTGCTTG	1457
IL1B	NM_000576	CAACAGGCTGCTCTGGGATTC	28	AGTCATCCTCATTGCCACTGT	131
IL6	NM_000600	TGGATTCAATGAGGAGACTTGC	433	GGGTCAGGGGTGGTTATTGC	608
IL8 (CXCL8)	NM_000584	TGCAGCTCTGTGTGAAGGTG	201	GGGGTGGAAAGGTTTGGAGT	272
TNF	NM_000594	TGGGATCATTGCCCTGTGAG	859	GGTGTCTGAAGGAGGGGGTA	931

Table I. Primer pairs for quantitative RT-PCR.

The position of each primer's 5'-terminal nucleotide within the mRNA is indicated. RNA18S5, 18S ribosomal RNA; POLR2A, RNA polymerase II subunit B1; COX2, cyclooxygenase 2; SIP, steroid receptor coactivator interacting protein; IL1B, interleukin 1B; IL6, interleukin 6; IL8, interleukin 8; CXCL8, chemokine (C-X-C Motif) ligand 8; TNF, tumor necrosis factor.

Supplementary tables and legends

Supplementary table I

Expt #	Accession	Description	Gene Name	Coverage (%)	# PSMs	# Peptides	Score
1	Q63ZY3	KN motif and ankyrin repeat domain-containing protein 2	KANK2	20.45	98	10	564.59
2	Q63ZY3	KN motif and ankyrin repeat domain-containing protein 2	KANK2	47.36	141	32	710.33
3	Q63ZY3	KN motif and ankyrin repeat domain-containing protein 2	KANK2	21.62	42	15	277.65

Supplementary table I. Mass spectrometry (MS) identification of steroid receptor co-activator interacting protein (SIP or KANK2) from 44-1085G immunoprecipitates (IPs), n=3.

A gel slice corresponding to the 100 kDa 'pMYLK' immunogen was subjected to in-gel digestion, peptide fractionation and tandem mass spectrometry analysis carried out on a LTQ-Orbitrap Velos mass spectrometer (see Methods). The raw data files were processed using Proteome Discoverer software v1.2 with searches performed against the UniProt Human database using the SEQUEST algorithm. The reverse database search option was enabled and all peptide data was filtered to satisfy false discovery rate (FDR) of 5%. KN motif and ankyrin repeat domain-containing protein 2 (KANK2) was the top hit when ranked by protein score after exclusion of keratin. Percentage sequence coverage, # peptide spectrum matches (PSMs) and # peptides matched are shown.

Supplementary table II

Sequence	Modifications	Phosphorylation site	Probability	XCorr	m/z [Da]	MH+ [Da]
AQ**S**LEPYGTGLR	S3(Phospho)	Serine 356	2.24	2.89	686.32	1371.64
VP**S**VAEAPQLRPAGTAAAK	S3(Phospho)	Serine 548	24.62	3.08	957.49	1913.99
ALAMPGRPE**S**PPVFR	M3(Oxidation) S10(Phospho)	Serine 375	31.55	2.94	852.92	1704.83
QADPQPQAWPPPD**S**PVRVDTVR	S14(Phospho)	Serine 323	1.37	3.43	846.07	2536.21

Supplementary table II. Peptides from SIP (KANK2) phosphorylated within 44-1085G IPs from forskolin-treated cells.

Following tandem mass spectrometry on a LTQ-Orbitrap Velos mass spectrometer (see Methods), the raw data files were processed using Proteome Discoverer software v1.2. Searches of the UniProt Human database using the SEQUEST algorithm included phosphorylation of serine, threonine and tyrosine as variable modifications. Specific phospho-peptides identified in a representative experiment are shown with the phospho-amino acid highlighted in bold, these were all identified at < 1 % FDR. Proteome Discoverer Probability Score, XCorr, mass to charge ratio (m/z) in daltons (Da) and precursor ion mass (MH+) of the individual peptides are shown.

Supplementary table III

Sequence	Modifications	Phosphorylation site	EGF			MH+ [Da]
			Probability	Xcorr	m/z [Da]	
ALAMPGRPE**S**PPVFR	M4(Oxidation) S10(Phospho)	Serine 375	7.22	3.26	860.91	1720.81731
QADPQPQAWPPPD**S**PVRVDTVR	S14(Phospho)	Serine 323	21.80	3.90	846.07	2536.19217

Supplementary table III. SIP (KANK2) peptides within SIP IPs phosphorylated in epidermal growth factor (EGF)-treated cells and absent in non-stimulated samples.

SIP (antibody ab99351) and control (normal rabbit IgG) IPs were performed from non-stimulated or EGF-stimulated myometrial cell lysates. IPs were resolved by gel electrophoresis, and subjected to in-gel digestion, peptide fractionation and tandem mass spectrometry analysis carried out on a LTQ-Orbitrap Velos mass spectrometer (see Methods). The raw data files were processed using Proteome Discoverer software v1.4 with searches performed against the UniProt Human database using the SEQUEST algorithm, including phosphorylation of serine, threonine and tyrosine as variable modifications. Peptides associated with SIP (KANK2) were filtered at 1% FDR and to select phosphorylated peptides present only in EGF-stimulated SIP IPs (absent in the non-stimulated SIP IP and control IPs). The two resulting phospho-peptides are shown with the phosphorylation site in SIP indicated; Proteome Discoverer Probability Score, XCorr, m/z and MH+ of the individual peptides are shown.

Supplementary table IV

TF	Mean	±	SEM	TF	Mean	±	SEM
SRF	14.47	±	3.96 ***	**NF1**	1.22	±	0.56
STAT2	14.10	±	8.40	**NR1I2**	1.20	±	0.53
YY1	12.84	±	6.37 *	**TR**	1.14	±	0.49
SMAD	8.81	±	2.52	**HNF4**	1.08	±	0.33
NR1I3	5.48	±	4.90	**Pax-5**	1.03	±	0.30
GR/PR	5.26	±	3.28	**STAT1**	1.02	±	0.65
NFKB	4.90	±	2.38	**NF-E2**	1.02	±	0.58
STAT5	4.32	±	2.11	**SATB1**	1.02	±	0.41
CEBPZ	4.26	±	2.15	**PPAR**	1.00	±	0.48
EGR	4.06	±	1.99	**TCF/LEF**	0.99	±	0.35
p53	3.35	±	1.80	**Ets**	0.99	±	0.34
STAT3	2.70	±	1.09	**ER**	0.98	±	0.34
SP1	2.53	±	1.61	**Pbx1**	0.94	±	0.37
E2F1	1.91	±	0.63	**C\EBP**	0.94	±	0.26
CREB	1.89	±	0.75	**CDP**	0.91	±	0.59
NFAT	1.85	±	1.29	**Pit**	0.89	±	0.56
IRF	1.65	±	0.59	**GAS/ISRE**	0.87	±	0.25
AP-1	1.53	±	0.53	**FAST-1**	0.85	±	0.25
TBP	1.46	±	0.52	**Myb**	0.84	±	0.24
OCT4	1.44	±	0.52	**ATF-2**	0.80	±	0.32
MEF2	1.42	±	0.35	**HIF**	0.79	±	0.56
GATA	1.34	±	0.47	**AP-2**	0.72	±	0.28
Myc-MAX	1.25	±	0.78	**AR**	0.63	±	0.18
STAT6	1.24	±	0.60				

Supplementary table IV. Transcription factor (TF) activation after SIP knockdown.

Primary myometrial cells were transfected with scrambled siRNA (SCR) or a combination of two SIP siRNAs (SIP). The activation of 47 TFs was assayed in nuclear extracts by their ability to bind their consensus DNA sequence, as per methods. Data are presented as fold activation in SIP relative to SCR (mean ± SEM, n = 3), and one-sample t-tests were performed against a constant of 1; *** $P < 0.001$, * $P < 0.05$. AP1, Activator protein 1 (JUN/FOS); AP2, Activator protein 2; AR, Androgen receptor; ATF2, activating transcription factor 2; Brn-3, POU domain, class 4, transcription factor 1; C/EBP, CCAAT/enhancer binding protein alpha; CEBPZ, CCAAT/enhancer binding protein (C/EBP), zeta; CDP, CCAAT displacement protein; CREB, cAMP responsive element binding protein 1; E2F1, E2F transcription factor 1; EGR, Early growth response; ER, Estrogen receptor; Ets, v-ets erythroblastosis virus E26 oncogene homolog 1; FAST-1, Forkhead box H1; GAS/ISRE, IFN-stimulated response element; GATA, GATA transcription factor; GR/PR, Glucocorticoid

receptor/Progesterone receptor; HIF, Hypoxia inducible factor; HNF4, Hepatocyte nuclear factor 4; IRF, Interferon regulatory factor; MEF2, Myocyte enhancer factor 2; Myb, v-myb myeloblastosis viral oncogene homolog; Myc-Max, v-myc myelocytomatosis viral oncogene homolog (avian); NF1, Nuclear factor 1; NFAT Nuclear factor of activated T-cells; NF-E2, Nuclear factor (erythroid-derived 2); NFKB, nuclear factor of kappa B; NR1I, nuclear receptor subfamily 1, group I; OCT4, POU class 5 homeobox 1; p53, Tumor protein p53; Pax-5, Paired box 5; Pbx1, Pre-B cell leukemia transcription factor-1; Pit, Pituitary specific transcription factor 1; PPAR, Peroxisome proliferator-activated receptor; PXR, Pregnane X receptor; SMAD, SMAD family; SP1, SP1 transcription factor, SRF, Serum response factor; SATB1, Special AT-rich sequence binding protein 1; STAT, Signal transducer and activator of transcription; TBP, TATA box binding protein; TCF/LEF, Runt-related transcription factor 2; TR, Thyroid hormone receptor; YY1, YY1 transcription factor.

Supplementary figure 1

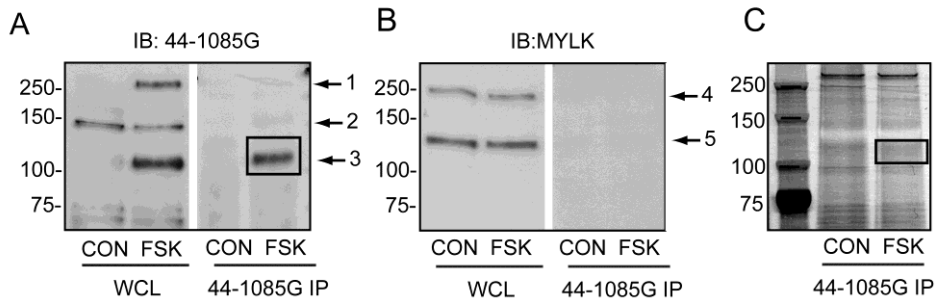

Figure 1

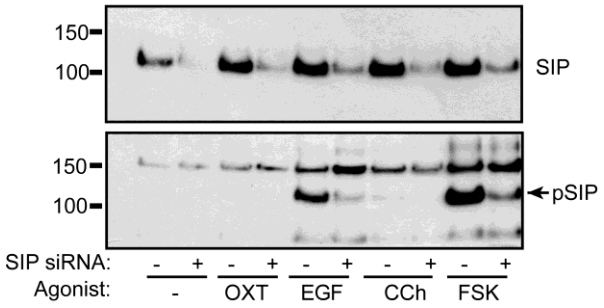

Figure 2

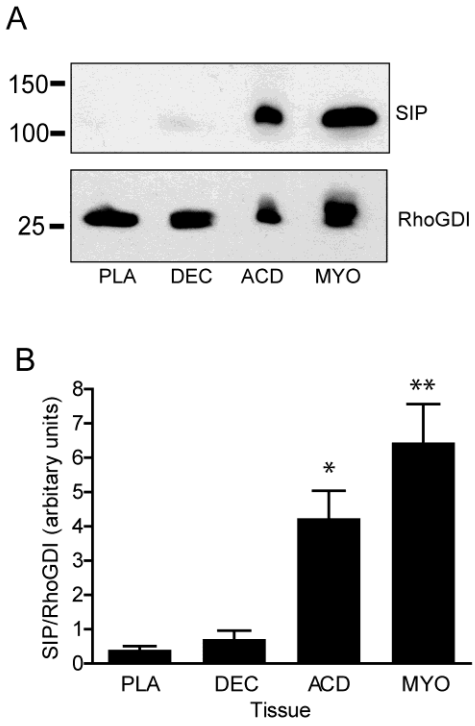
A
150
100
SIP
25
RhoGDI
PLA
DEC
ACD
MYO
B
SIP/RhoGDI (arbitary units)
0
1
2
3
4
5
6
7
8
*
**
PLA
DEC
ACD
MYO
Tissue

Figure 3

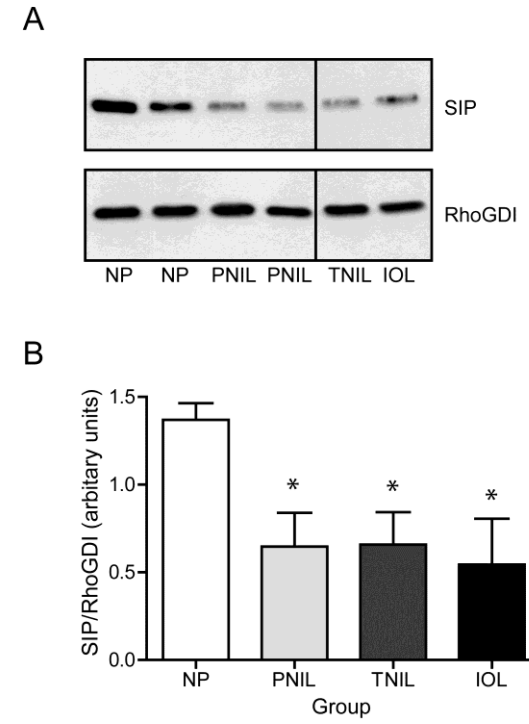

Figure 4

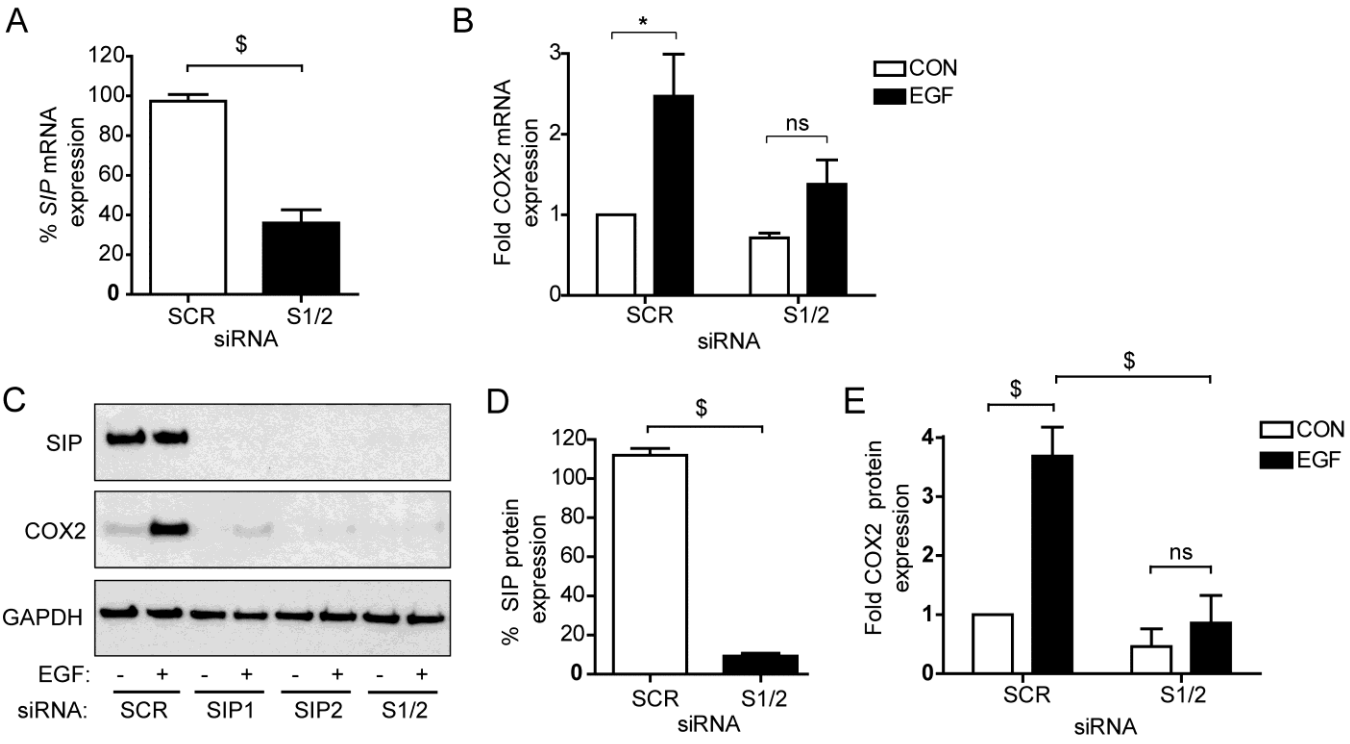

Figure 5

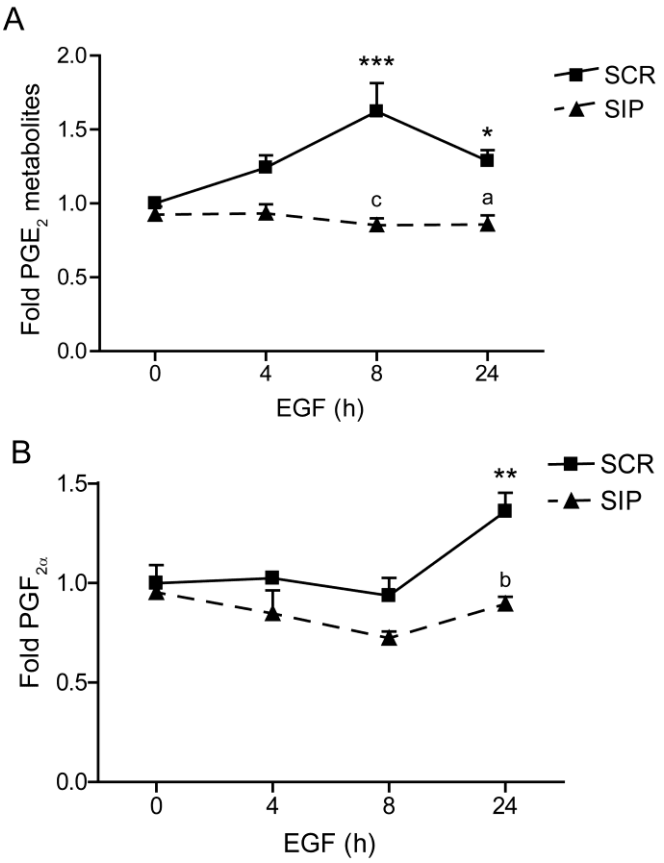
A
2.0
1.5
1.0
0.5
0.0
Fold PGE2 metabolites
***
*
c
a
SCR
SIP
0
4
8
24
EGF (h)
B
1.5
1.0
0.5
0.0
Fold PGF2α
**
b
SCR
SIP
0
4
8
24
EGF (h)

Figure 6

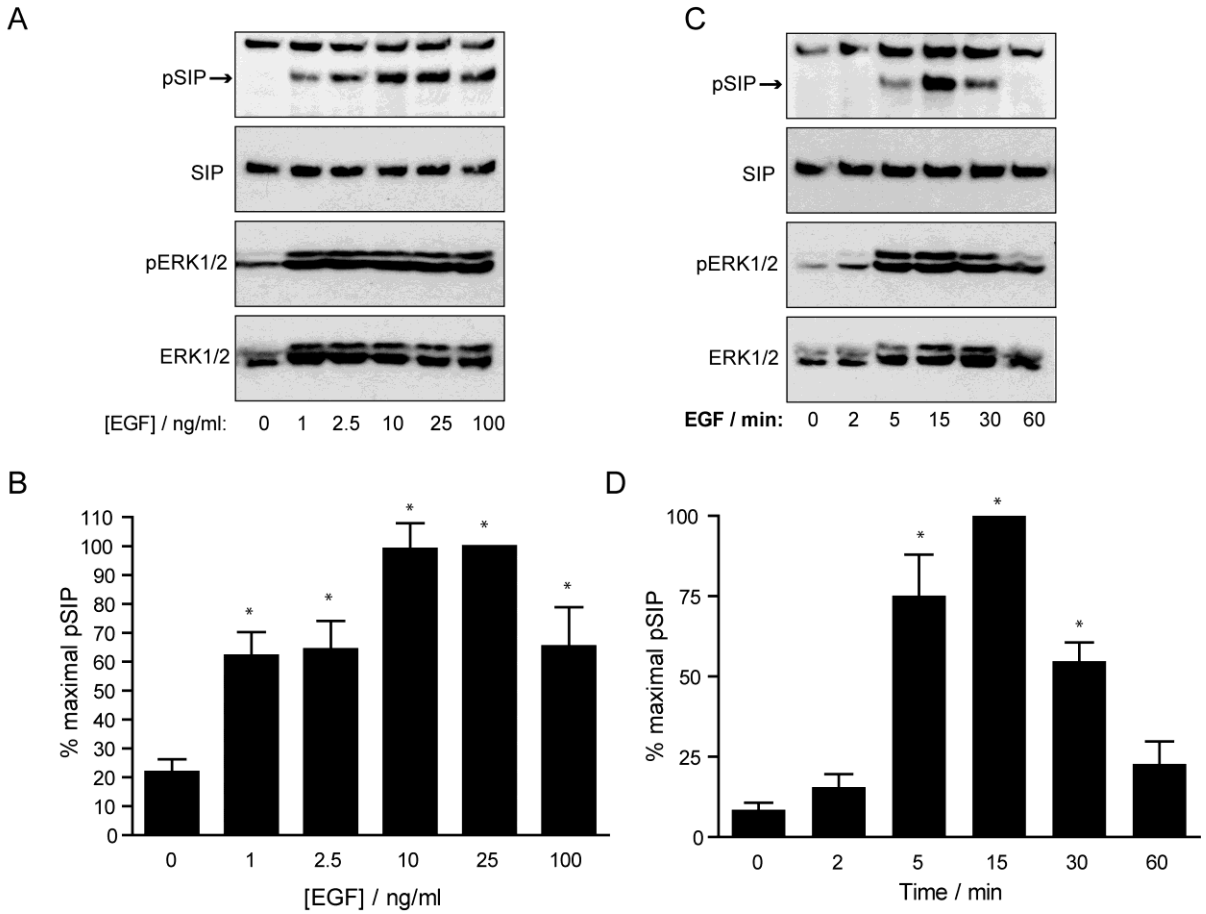
A
pSIP
SIP
pERK1/2
ERK1/2
[EGF] / ng/ml: 0 1 2.5 10 25 100
C
pSIP
SIP
pERK1/2
ERK1/2
EGF / min: 0 2 5 15 30 60
B
% maximal pSIP
0 1 2.5 10 25 100
[EGF] / ng/ml
D
% maximal pSIP
0 2 5 15 30 60
Time / min

Figure 7

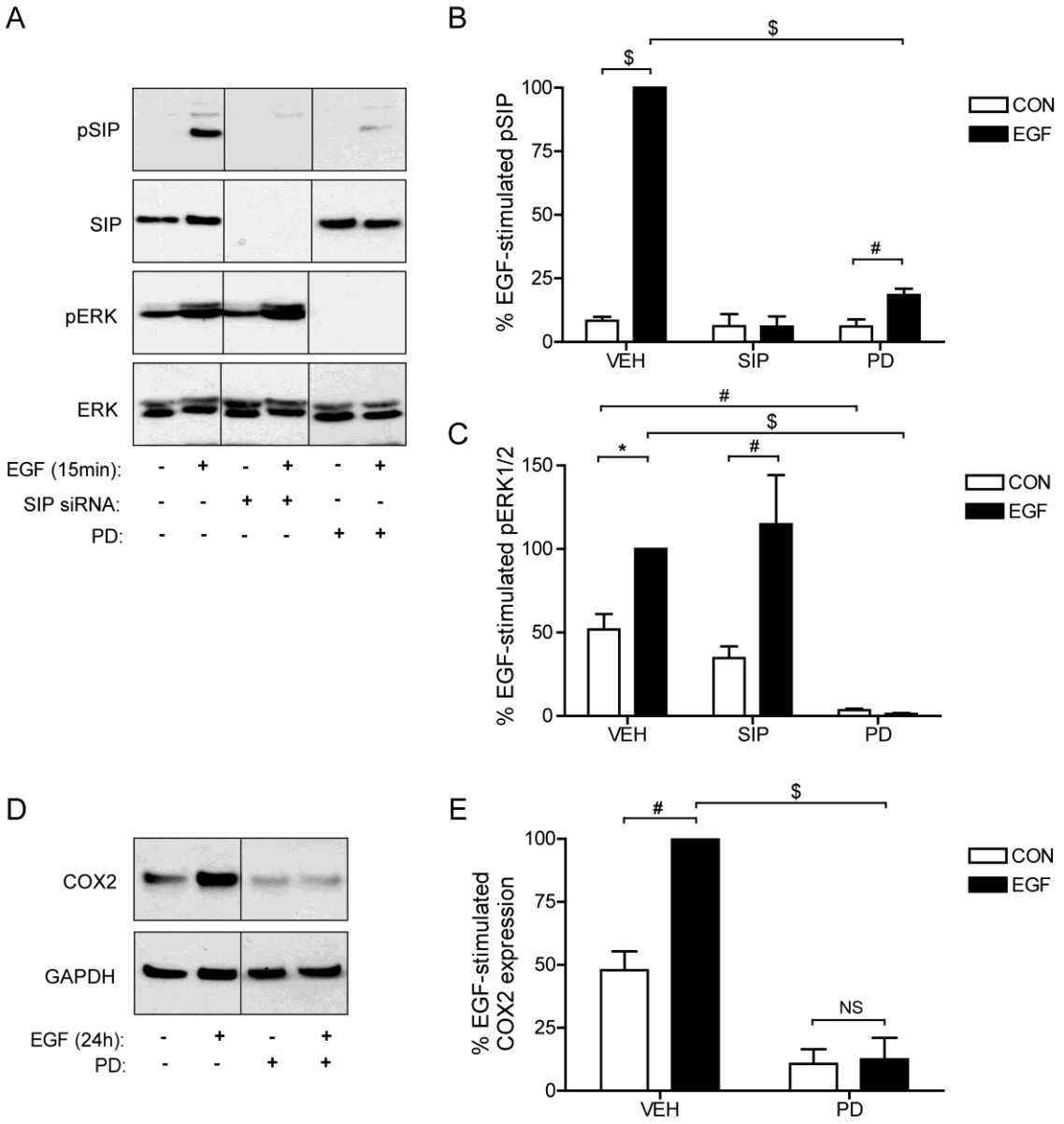
A
pSIP
SIP
pERK
ERK
EGF (15min): - + - + - +
SIP siRNA: - - + + - -
PD: - - - - + +
B
% EGF-stimulated pSIP
100
75
50
25
0
$
$
#
VEH
SIP
PD
CON
EGF
C
% EGF-stimulated pERK1/2
150
100
50
0
#
$
*
#
VEH
SIP
PD
CON
EGF
D
COX2
GAPDH
EGF (24h): - + - +
PD: - - + +
E
% EGF-stimulated COX2 expression
100
75
50
25
0
#
$
NS
VEH
PD
CON
EGF

Figure 8

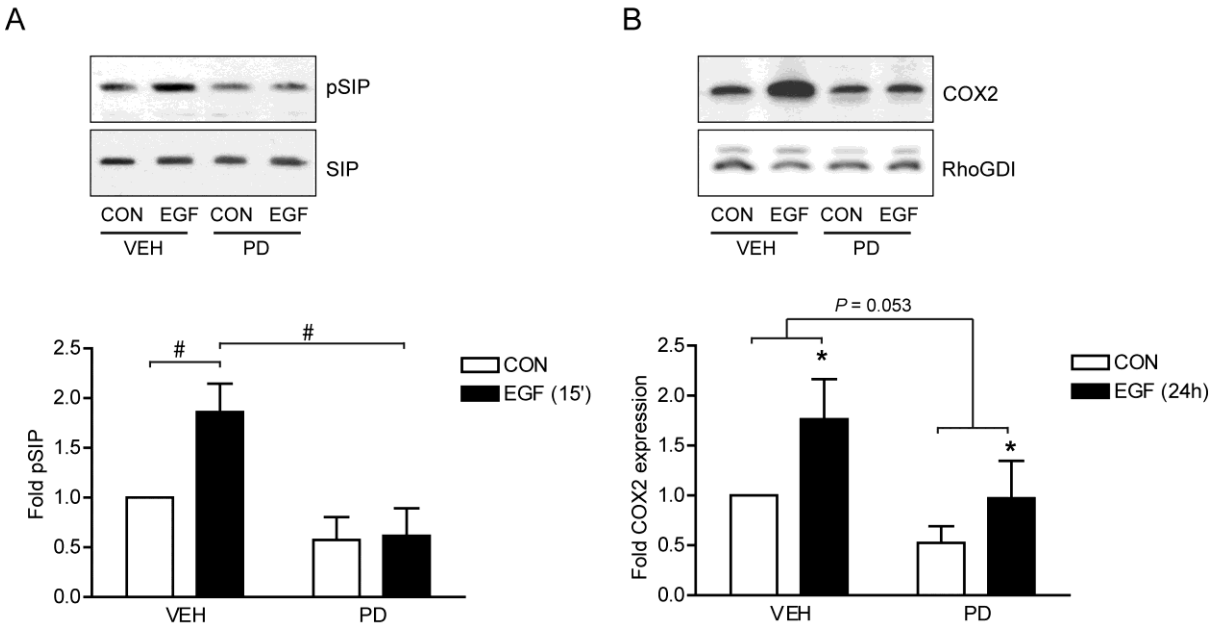
A
pSIP
SIP
CON EGF CON EGF
VEH PD
Fold pSIP
2.5
2.0
1.5
1.0
0.5
0.0
#
#
VEH
PD
CON
EGF (15')
B
COX2
RhoGDI
CON EGF CON EGF
VEH PD
P = 0.053
Fold COX2 expression
*
*
CON
EGF (24h)

Figure 9

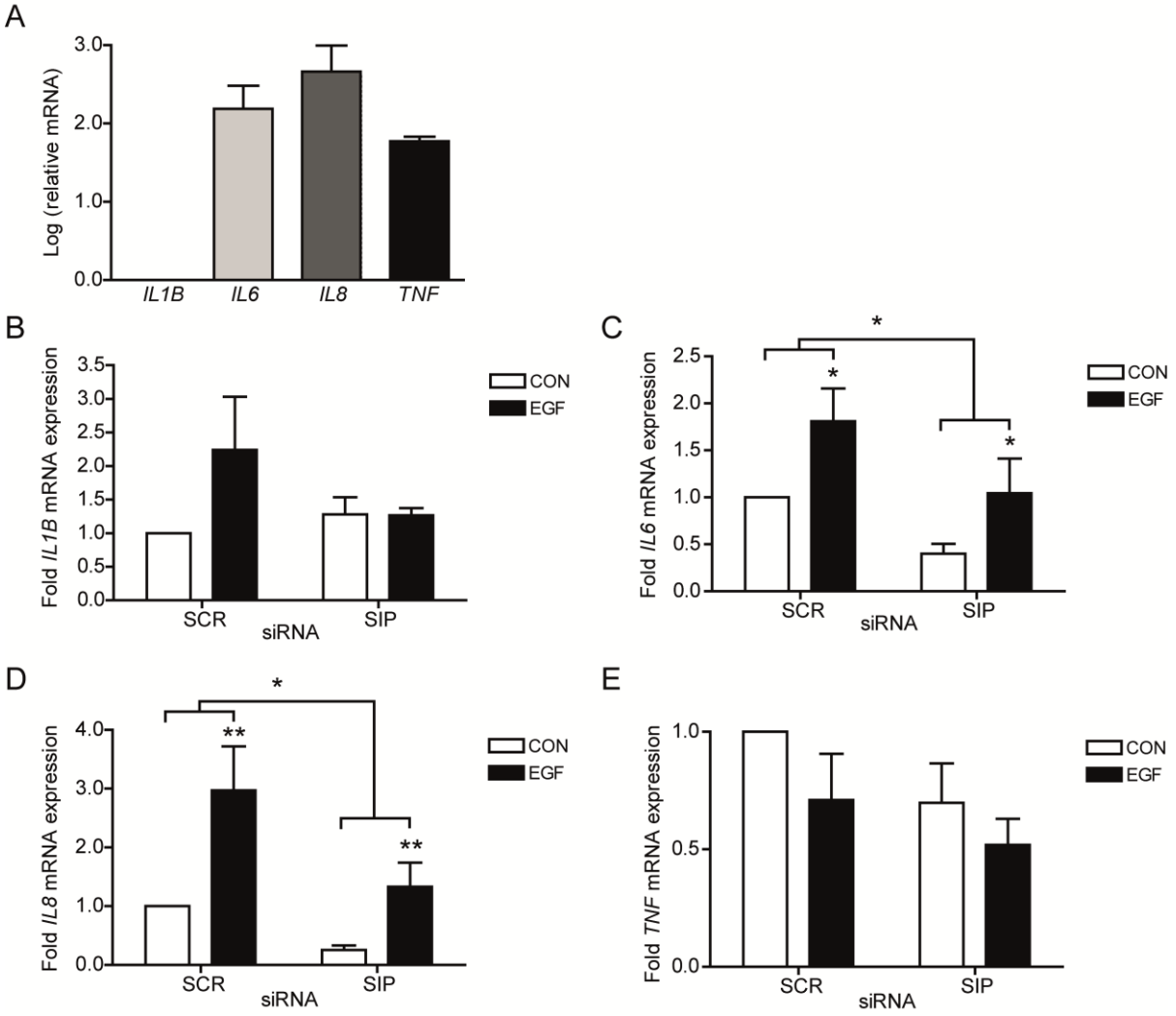
A
Log (relative mRNA)
3.0
2.0
1.0
0.0
IL1B
IL6
IL8
TNF
B
Fold IL1B mRNA expression
CON
EGF
SCR
siRNA
SIP
C
Fold IL6 mRNA expression
*
D
Fold IL8 mRNA expression
**
E
Fold TNF mRNA expression

Figure 10

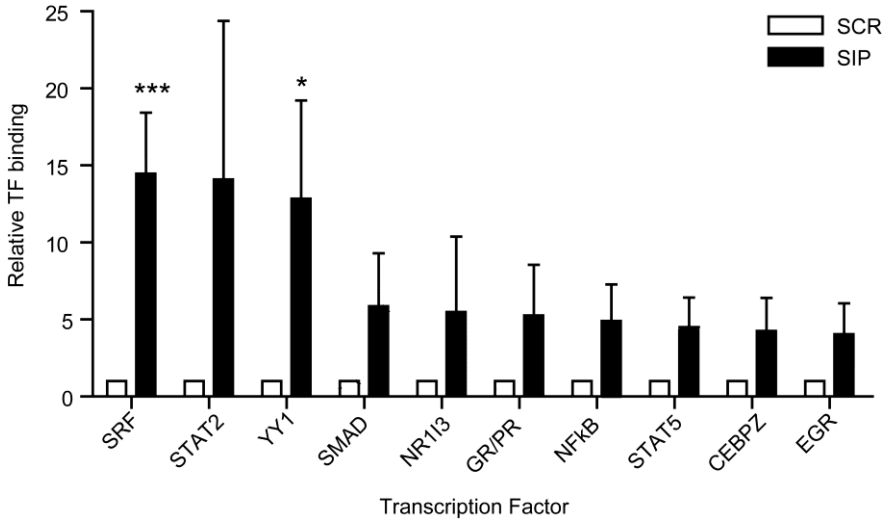

Figure 11